Supporting Information

Mechanism and Stereochemistry of Polyketide Chain Elongation and Methyl Group Epimerization in Polyether Biosynthesis

Xinqiang Xie,[†] Ashish Garg,[†] Chaitan Khosla,[§] and David E. Cane[*,†]*

[†]Department of Chemistry, Box H, Brown University, Providence, Rhode Island 02912-9108

[§]Departments of Chemical Engineering, Chemistry, and Biochemistry, Stanford University, Stanford, California 94305

*To whom correspondence should be addressed: david_cane@brown.edu

Table of Contents

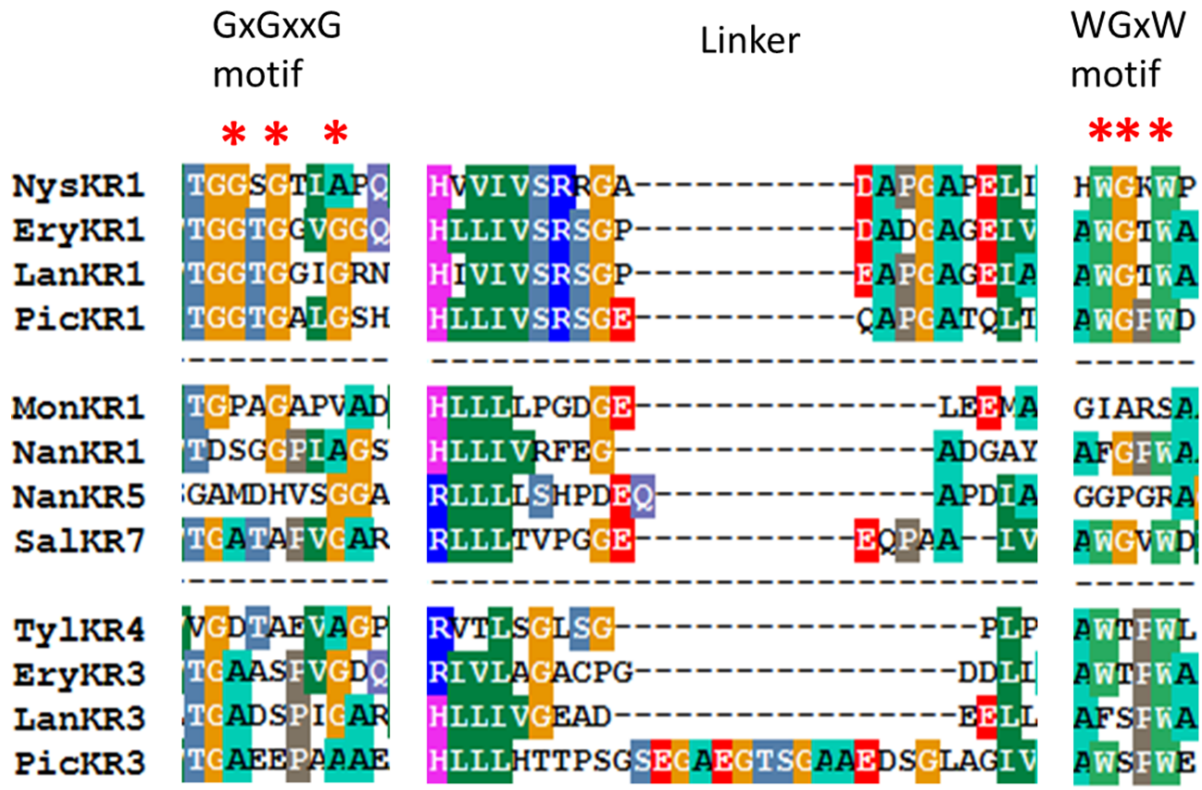

Figure S1. Mega3.0 (http://www.megasoftware.net) sequence alignment of NADPH binding site motifs, GxGxxG, WGxW, and the intervening linker region, for redox-active, epimerase-active KR domains (rows 1-4) and redox-inactive, epimerase-active KR^0 domains (rows 9-12) with presumptive redox-inactive, epimerase-active KR^0 domains from polyether synthases (rows 5-8). PKS source: Ery, erythromycin; Lan, lankamycin; Mon, monensin; Nan, nanchangmycin; Nys, nystatin; Pic, picromycin; Sal, salinomycin; Tyl, tylosin.

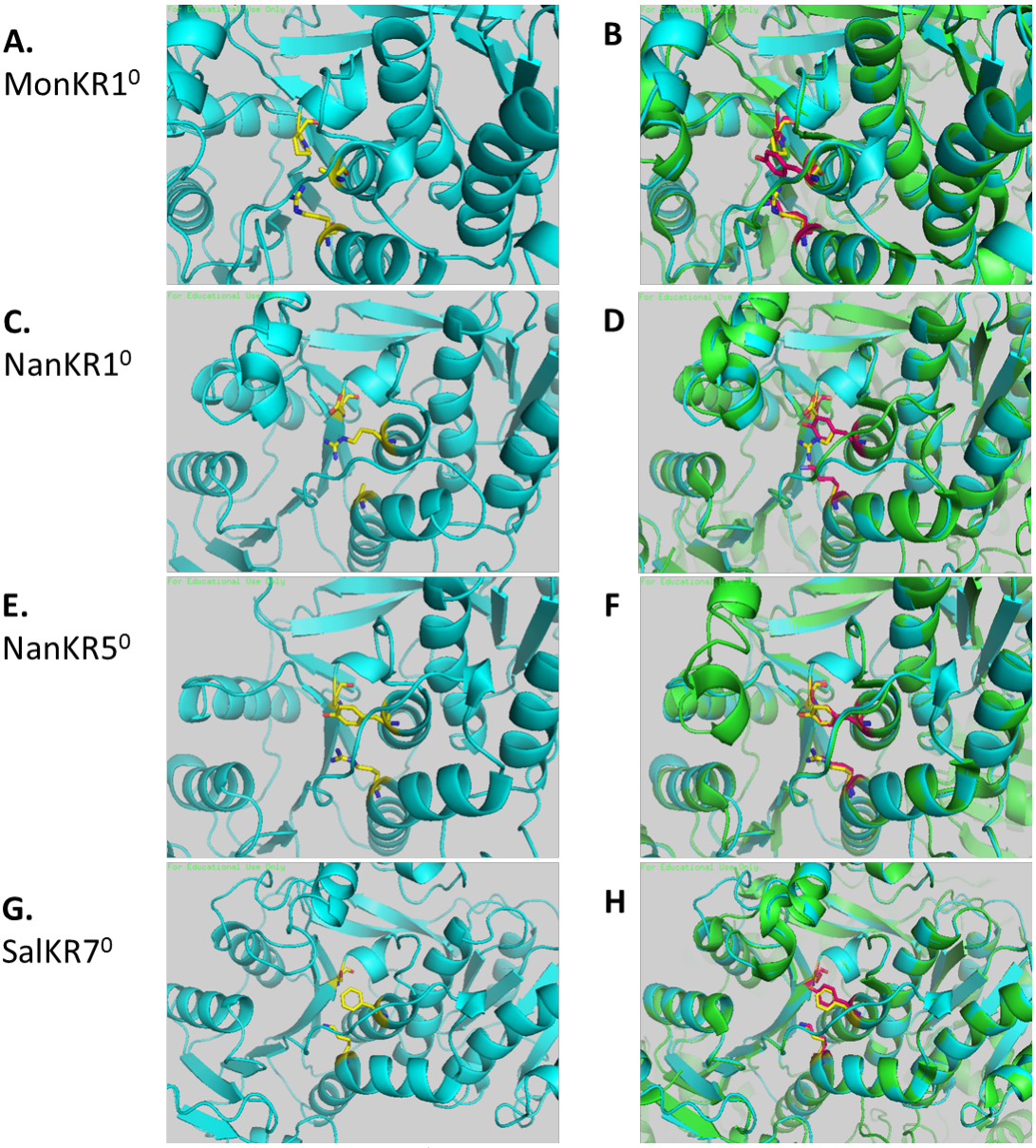

Figure S2. SWISS-MODEL[1] (https://swissmodel.expasy.org/) protein structure homology-models of KR^0 domains from polyether synthases, generated using the PicKR3 structure (PDB number: 3QP9) as template. A. Predicted active site of $MonKR1^0$ protein structure model based on $PicKR3^0$ structure; B. Protein structure overlap of $MonKR1^0$ with $PicKR3^0$; C. Predicted active site of $NanKR1^0$ protein structure model based on $PicKR3^0$ structure; D. Protein structure overlap of $NanKR1^0$ with $PicKR3^0$; E. Predicted active site of $NanKR5^0$ protein structure model based on $PicKR3^0$ structure; F. Protein structure overlap of $NanKR5^0$ with $PicKR3^0$; G. Predicted active site of $SalKR7^0$ protein structure model based on $PicKR3^0$ structure; H. Protein structure overlap of $SalKR7^0$ with $PicKR3^0$.

LOCUS AAP42855 2902 aa linear BCT 23-MAY-2003

DEFINITION NanA1 [*Streptomyces nanchangensis*].

ACCESSION AAP42855

VERSION AAP42855.1 GI:31044143

DBSOURCE accession AF521085.1

1MRFRYGGVMAGSSPSHAQQATSPVAIVGLACRLPGAPDPEAFWRLLRAGENAVVPVPDSR

(.....Nanchangmycin PKS loading module.....)

1021AAWLRAAHEGQPTAAPTAATGPSMAEDPVAVVAVSCRYPGGVESGEALWRLVDEGVDAVG

1081EFPGDRGWDLAELFGRAPDGSGGSATGRGGFLYGAGDFDAEFFGISPREALAMDPQQRIL

1141LELSWELLERAGIPPASLAGSATGVYVGATAVDYGPRLHEATAELDGHLLTGSTPSVASG

1201RVAYALGLEGPALTVDTACSSSLVAMHLAAQALRQGECDLALAGGVTVMATPGMFTSFSR

1261QRGLAPDGRCKPFAAAADGTGWSEGAGLVLLERLSDARRNGHQVLAVIRGSAVNQDGASN

1321GLSAPNGPSQQRVIRQALANARLEPADVDAVEAHGTGTTLGDPIEAQALLATYGGQRTDD

1381RPLWLGSIKSNIGHTQAAAGVAGVIKMVMALRHGRLPASLHIDAPSPHIDWSDGTVRLLS

1441EPVDWPGTDWPGSDRPRRAAVSSFGISGTNAHLILEQAPDHPEPEPTTSGGVVPWVLSAR Nan[KS1][AT1]

1501TADALRAQAGRLAEWVTAGAPRSPASPTSPASPADVGWSLATTRSADRHRAVVSGTDRDE

1561LLSGLRAVADGLAPAAVSAGAAPGPVMVFPGQGSQWRGMGVELLDSSPVFAARMAACEAA

1621LGEFVDWSLTAVLRGAPGAPEPSRVDVLQPCLWAVMVSLAAVWESYGVTPTAVVGHSQGE

1681IAAACVAGGLSLRDGARVVALRSQALRALAGHGTMASLALSGAEAERFLADLGAAAARVT

1741VAVFNGPYSTVVSGPTDQVAAVVAACEAAGHRARTIDVDYASHGPQVDRLADTIRTDLAD

1801LSPGASDAVFYSAVTGARQPTEELDADYWFTNLRQPVRFASAIDALLAAGYRVFIEVSPH

1861PVLIPALRECFEEAEVAAATVPTLRRDQGGPDQVARALGDGFVAGLAVDWSRWFVGDGRE

1921AGDEGHRPRTVELPTYPFQRRRYWLAPDHGRREGRTAGVGTRPAGHALLSSAVELADGGL

1981VLSGRLPGDAAWVGAHTVAGVQLVPGAVLVDWALLAADEAGGASLEELLLRAPLELSGPS

2041GLSEPSAGVLAQVAVGAPDESGRRELRISSRPADAGAGEGWTCHAVGSLAPGGPPAPADT

2101GTATVPWPPAGAEALDPAGLYERAERRGYGYGPALRGVVALWRDGADLVADVALPEEAGG NanDH1

2161GGEGGADGDGTAGFGLHPVLLDAALQPALLAEPDGTGGEGAGPEARLWLPFAWSGVRLWA

2221TGARAARVRLSPLDGGGGDVADERELRIEVSDPTGAPVLSVASVVLRPRTVRQVREASGA

2281AAGGLFALDWTPVAPQEPSGAEDDAGCVAVLGEAPTEPGVDGCRDTYTDLPALLAALDAG

2341APLPSVVMWRPPAADPGAAPEDAALSAVRGVAAALRAWVAEPRLTVSRLAVVTRGAVAAG

2401GAEGEPVDLAAAAAWGCARGVQAEHPDRIVLVDVDDDVDMGADTDTDIGAAAGLAAALGE

2461PQVALRGDTLLAPRLARSAATPGGVAFDPNGTVLVTDSGGPLAGSVAEHLVRAEGVRHLL NanKR1^{0}

2521LVRFEGADGAYDTYDRQDAQVHMVTVDPRDTAALERVVAQVDPAHPLTGVVHVAGLSADI

2581ETSGAARGWAVAAGVVRALHQATAALPSVRFVTLSDAATAWDGPAAPERAAAGAFCAAVT

2641DVRRRAGLHGLDVAFGPWAAADDDGGADSGGRWTGVLGADRGLALLRAACRADRPRLVAA

2701DIRTRALTAHPAHELPAALRTLGASASASASAGGRAPVRRVAAAAPGRTTDWASRLVGLGPA

2761ERRRAVLELVRDHAAAVLGQPDPKAVRADASFKELGFDSVTAVELRDRLVAVGGLRLPAA

2821VVFRHPTPEALAHRIEQQLAPDDTNNAAITDNADNAAKSNGNSNGTALDAADKLASATAD NanACP1

2881EILDFIDNELGVLSEARPRPSN

Figure S3. Domain boundaries of nanchangmycin synthase module 1 and design of recombinant Nan[KS1][AT1], NanACP1 and NanKR1^{0}

LOCUS CCD31893 1642 aa linear BCT 03-FEB-2012
DEFINITION type I modular polyketide synthase [*Streptomyces albus* subsp. albus].
ACCESSION CCD31893
VERSION CCD31893.1 GI:373248780
DBSOURCE embl accession HE586118.1

1 MDNEKKLLDHLKWVTAELRQARQKLREAEADEPEPIAIVSMACRYPGGVRSPEDLWQLVR
61 EGRDAITGFPTGRGWDLASLYDADPDRLGTSYVREGGFVHDAGDFDAEFFGISPREALAM
121 DPQQRLLLETSWEAFERAGVDPAAVAGSRTGVFVGTTYTGYGSDREGAEENVEGHLMTGI
181 ATAVASGRLSYTYGFEGPAVSLDTMCSSSLVALHLAVQALRQKECTLALAGGSQIMSTPD
241 VYVEFSRQRGLSPDGRCKPFAAAADGTGWSEGVGVLLLERLSDARRNGHRVLAVVRGSAI
301 NQDGASNGLTAPNGPSQQRVIEQALANARLSPHQVDLIEAHGTGTTLGDPIEAQALLATY
361 GGSRPEGRPLWLGSVKSNIGHAAAAAGVAGVIKAVMAVREGVLPKSLHIDAPTPEVDWSS
421 GAVALLTEEREWSVPGEEPRTAAISSFGASGTNAHVLVQYAPEPDPEPAAEAPAAVFTGA Sal[KS7][AT7]
481 ALPWLLSGRTAEGLRGQARSLHTYASTTATALPGAALGLATTRAALERRGAVLTSGTPGT
541 PDKDALLTGLDALAEGTPAAGILEGTTVSGADRPVFVFPGQGSQWAGMAVELLDSSSVFA
601 ARLGECAEALDPFVDWSLVDVLRQTEGAPGFDRVDVVQPALWAVMVSLAEVWRAAGVAPA
661 AVIGHSQGEIAAAAVSGALSLSDAAKVSALRARALLALAGKGGMVSVADAADSVRERISA
721 WGERLALASVNGPQSTVVSGDPEALDELMAGCEAEGVRARRINVDYASHGPQVEKIRTEV
781 LGALSGIEPRTAEVPFLSTVTGEFVTGTELDAEYWYRNLRNTVRFEDAVRQLLDRGHGAF
841 VEASAHPVLTVGVQETIDAAGAPAFVQGTLRREDGDAARFLASLAEAWTRGVPVNWAIVT
901 DSSAPPAEDLPTYAFQRRTYWLHGARTGSVQAPVDAVEAEFWDSVENGDIDSLSGSLALE
961 DSAPLAELLPALSSWRRRRRERGEVDSWRYRIDWQPLAESAPPALEGTWLLVTGDGVEAE
1021 ILKTGESALSAHGATVHPLTLTGEGEREALVRQLLGAEVEHGPFAGVLSLLATAEPERGP
1081 ATTLALVQALADAECEAPLWVATRGAVGTGPEEAPAHPAQAGAWGLGLVAALERPGGWGG
1141 LVDLPAEPDENLAGRLAAALAGQEDQLALRATGTYVRRLARAPLPGSEVRPWEPADTVLV SalKR7^0
1201 TGATAPVGARTALLLAASGAKRLLLTVPGGEEQPAALVGELEEAGVQVTLAEWDGRDVTA
1261 LRSLAEAAAADGAPVRGVFHAATRADLAPLDETTAADLAAATAAKTVPARALDEAFGEEV
1321 EAFVLFSSVTSYWGGGEHAAFAAASAELDALAARRRSRGLAATSVAWGVWDLFDAEQNPA
1381 EAAELQARSADRGLPLLDPETAWQALRLSLGRQETAIAVADVDWERFWPLFTSARPAPLL
1441 SDLPEVRGLGRGLAEDTGTGADPGAAEALRSKLAGLSPAEQDRALTDLVCAHAAAVLGHS
1501 SAGAVDAERAFKDLGFDSLTAVGLRNGLGAATGLSLPATLVFDYPTPAAMAGYVRDHLLA SalACP7
1561 GARQEATAAGVQSGLDQLEADLLSVALDKDERKNLTRRLEGLLSRFKDAQAAADEESVSG
1621 KLDSASDEEIFAFIREEFGRPE

Figure S4. Domain boundaries of salinomycin synthase module 7 and design of recombinant SalKR7^0

RGEVDSWRYRIDWQPLAESAPPALEGTWLLVTGDGVEAEILKTGESALSAHGATVHPLTLTGEGEREALVRQLLGAEVEHGPFAGV

LSLLATAEPERGPATTLALVQALADAECEAPLWVATRGAVGTGPEEAPAHPAQAGAWGLGLVAALERPGGWGGLVDLPAEPDENLA

GRLAAALAGQEDQLALRATGTYVRRLARAPLPGSEVRPWEPADTVLVTGATAPVGARTALLLAASGAKRLLLTVPGGEEQPAALVG

ELEEAGVQVTLAEWDGRDVTALRSLAEAAAADGAPVRGVFHAATRADLAPLDETTAADLAAATAAKTVPARALDEAFGEEVEAFVL

FSSVTSYWGGGEHAAFAAASAELDALAARRRSRGLAATSVAWGVWDLFDAEQNPAEAAELQARSADRGLPLLDPETAWQALRLSLG

RQETAIAVADVDWERFWPLFTSARPAPLLSDLPEVRGLGRGLAEDTGTGADPG

(N terminal *NdeI* site)

CATATGCGCGGTGAAGTGGATAGCTGGCGTTACCGTATTGACTGGCAACCGCTGGCGGAGAGCGCCCCTCCAGCCTTGGAAGGCAC

GTGGCTGCTGGTCACCGGCGATGGCGTCGAGGCTGAGATCCTGAAAACGGGCGAGAGCGCGCTGTCGGCACATGGCGCGACGGTTC

ACCCGCTGACCCTGACGGGTGAGGGTGAGCGTGAGGCACTGGTTCGCCAGCTGCTGGGTGCTGAAGTTGAACACGGCCCGTTTGCG

GGCGTGCTCTCTTTATTGGCGACCGCAGAGCCAGAGCGTGGTCCGGCGACGACGCTGGCACTGGTCCAAGCGCTGGCGGATGCGGA

GTGCGAGGCCCCGCTGTGGGTCGCGACCCGTGGTGCGGTGGGCACCGGTCCGGAAGAAGCGCCGGCGCATCCGGCGCAGGCTGGTG

CGTGGGGTCTGGGCCTGGTCGCAGCGCTTGAACGCCCGGGTGGCTGGGGTGGCCTGGTCGATCTGCCGGCGGAACCGGACGAGAAC

TTGGCGGGTCGTCTGGCCGCGGCGCTGGCCGGCCAGGAAGATCAGTTGGCGCTGCGTGCCACCGGCACGTACGTTCGCAGACTGGC

ACGCGCACCGCTGCCGGGTTCCGAAGTCCGTCCGTGGGAGCCTGCGGACACCGTTCTGGTGACTGGTGCGACCGCTCCGGTTGGTG

CTCGTACGGCCCTGCTGCTGGCTGCGTCTGGCGCAAAGCGTTTGCTGCTGACGGTTCCGGGTGGCGAGGAACAACCGGCGGCGCTG

GTTGGTGAACTGGAAGAGGCCGGTGTGCAAGTGACCTTGGCCGAGTGGGACGGCCGTGACGTTACCGCGCTGCGTAGCCTGGCAGA

GGCTGCCGCTGCGGACGGTGCGCCGGTCCGCGGTGTGTTTCACGCGGCGACGCGTGCCGATCTGGCCCCGCTGGACGAAACCACGG

CAGCGGACCTGGCTGCAGCGACCGCAGCCAAGACCGTGCCAGCGCGCGCGTTAGATGAAGCATTTGGTGAGGAAGTTGAGGCATTC

GTCCTGTTCAGCAGCGTTACCAGCTATTGGGGTGGCGGCGAGCACGCGGCGTTTGCAGCCGCAAGCGCAGAGCTGGACGCGCTGGC

AGCGCGTCGTCGTAGCCGTGGTTTGGCGGCAACCAGCGTAGCGTGGGGCGTCTGGGACCTGTTCGACGCTGAGCAGAATCCGGCAG

AGGCCGCAGAACTGCAGGCGCGTAGCGCTGACCGTGGTCTGCCGCTGCTGGATCCTGAAACCGCATGGCAGGCTTTGCGTCTGAGC

CTGGGTCGCCAAGAAACCGCGATCGCAGTTGCAGATGTGGATTGGGAACGCTTCTGGCCGTTGTTCACCTCCGCACGCCCGGCGCC

ACTGCTGAGCGATCTGCCTGAAGTGCGCGGTCTGGGCCGTGGTCTGGCCGAGGATACCGGTACTGGTGCGGATCCGGGT**TAA**CTCG

AG

(Stop codon and C-terminal *XhoI* site)

Figure S5. *SalKR7^0 amino acid sequence.* The synthetic gene encoding SalKR7^0 domain was subcloned into the corresponding *NdeI* and *XhoI* digested pET-28a vector and the recombinant protein was expressed with N-terminal His6-tag in *E.coli* BL21 (DE3). Protein expression and purification procedures are described below.

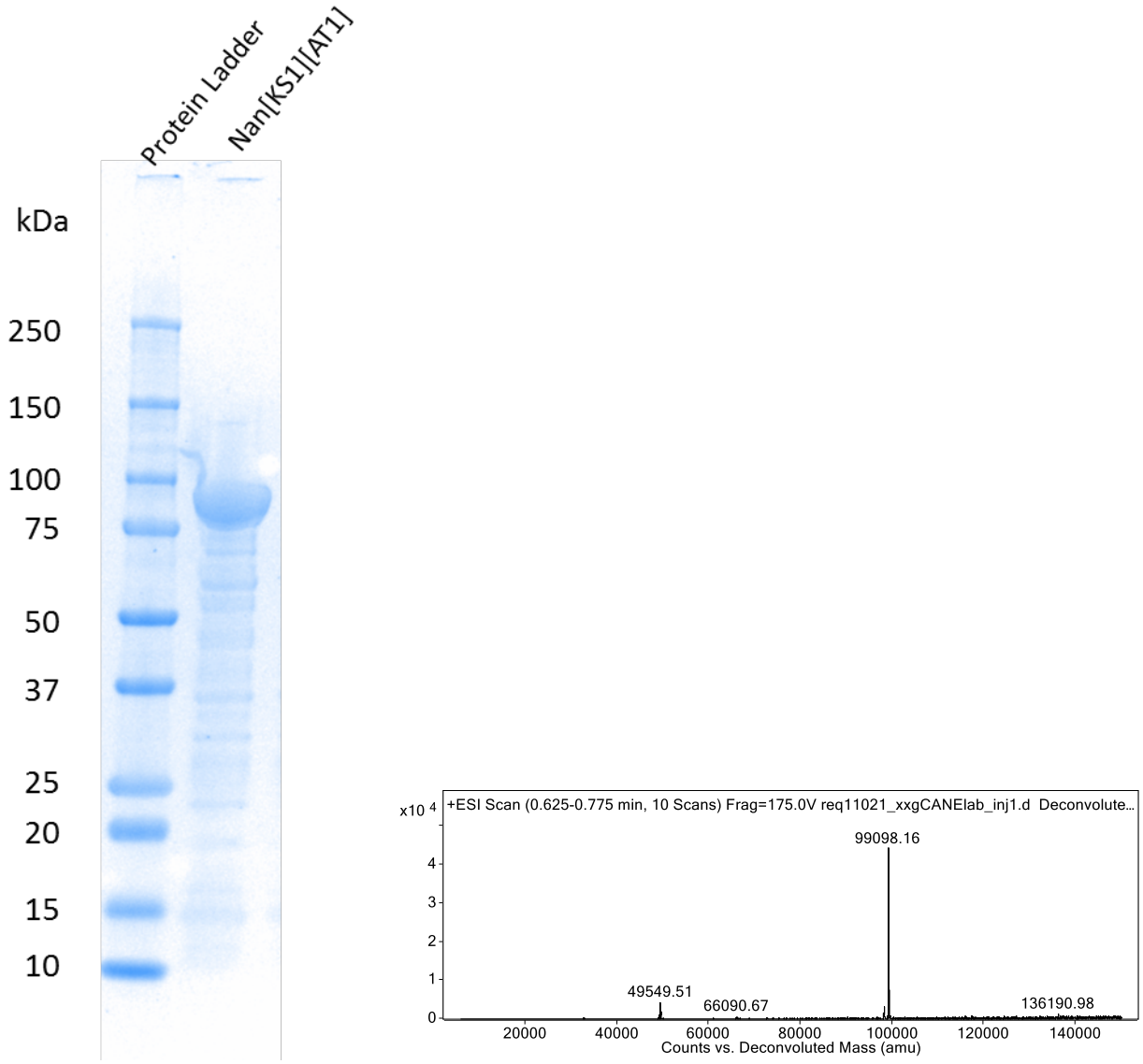

Figure S6. SDS-PAGE and LC-QTOF-MS analysis of recombinant Nan[KS1][AT1].

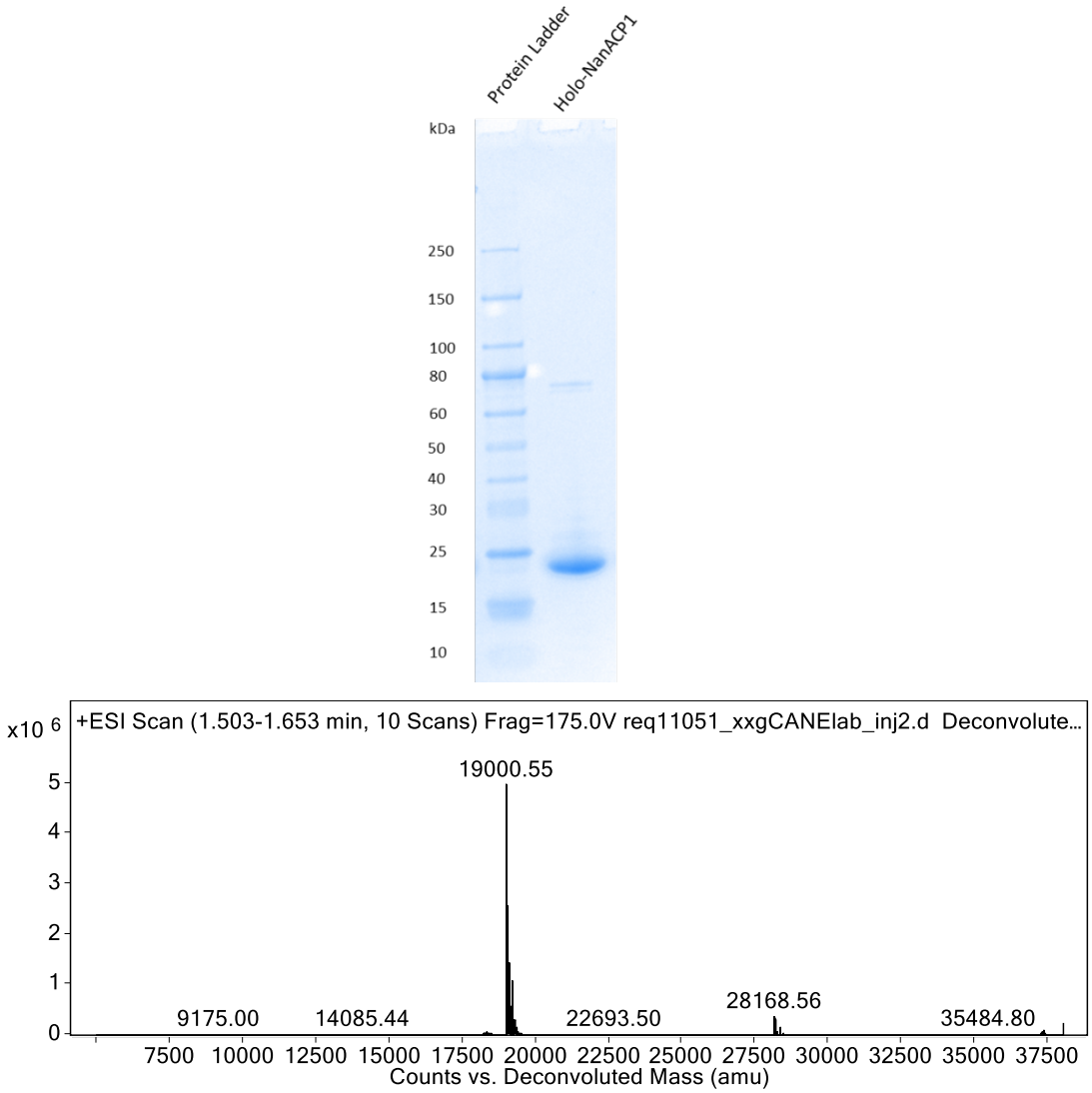

Figure S7. SDS-PAGE and LC-QTOF-MS analysis of recombinant holo-NanACP1.

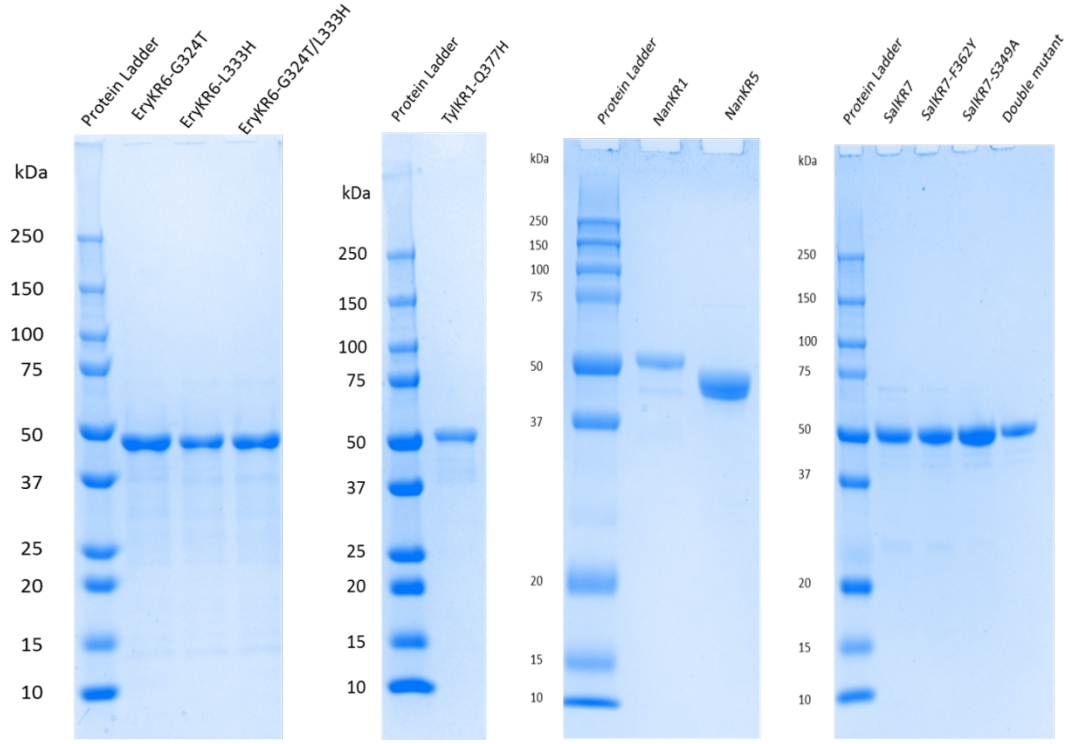

Figure S8. SDS-PAGE analysis of recombinant ketoreductases and mutants.

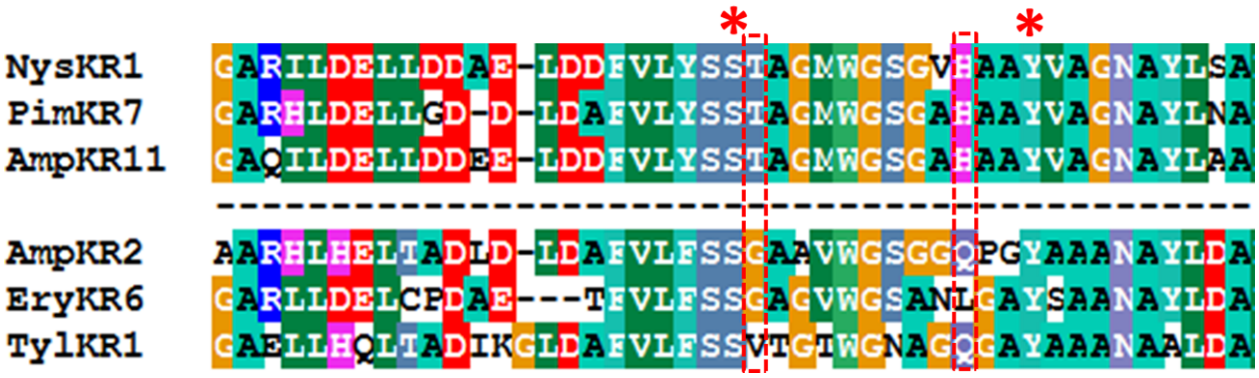

Figure S9. Alignment of epimerase-active KR domains (rows 1-3) with epimerase-inactive KR domains from polyketide synthases (rows 4-6). The conserved amino acids of Thr and His in epimerase-active KR domains are in broken red rectangles. (Pim, Pimaricin)

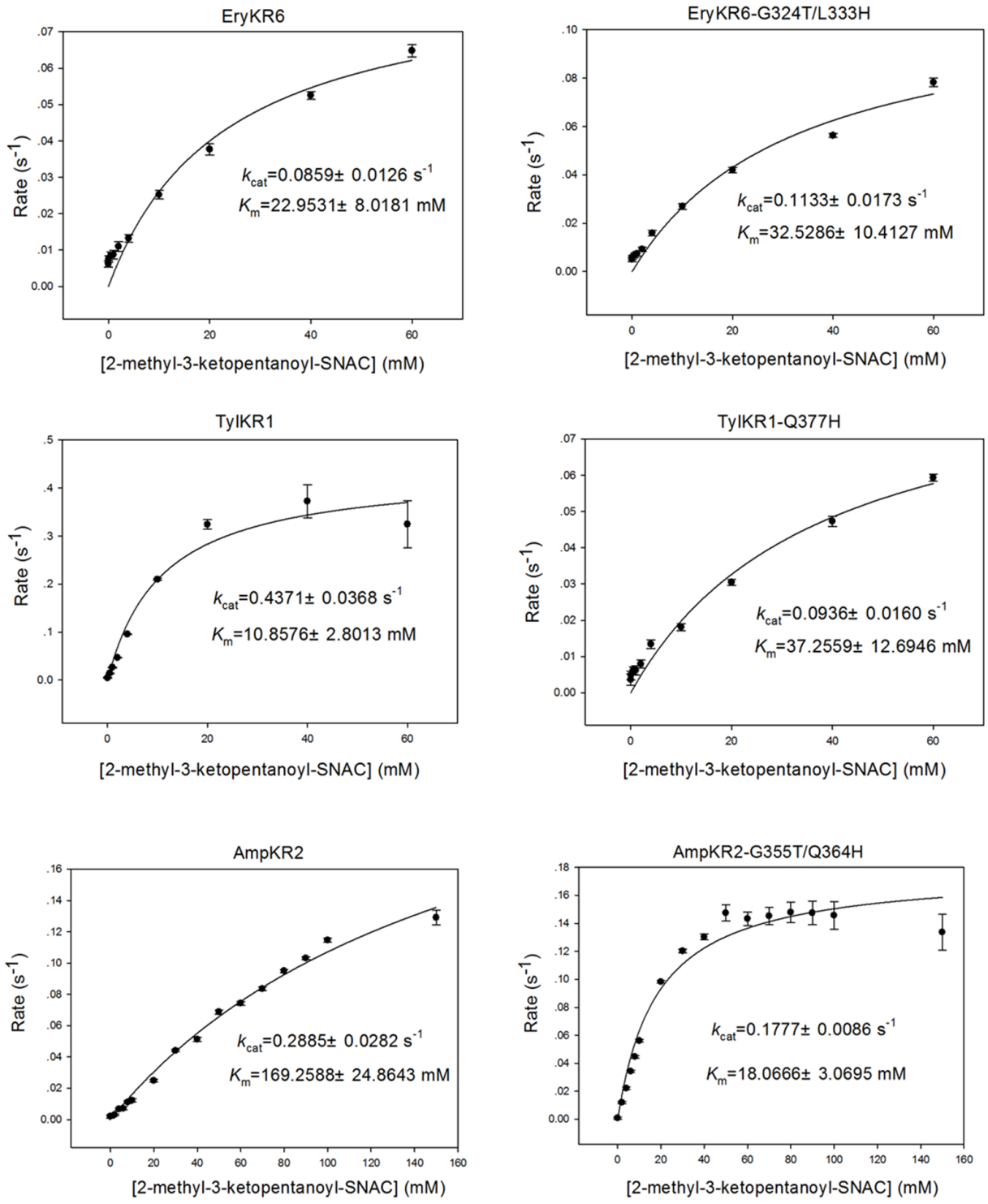

Figure S10. Ketoreductase activity of wild-type and mutant KR proteins for reduction of (±)-2-methyl-3-ketopentanoyl-SNAC (**5**). See Table S5 for summary of steady-state kinetic parameters.

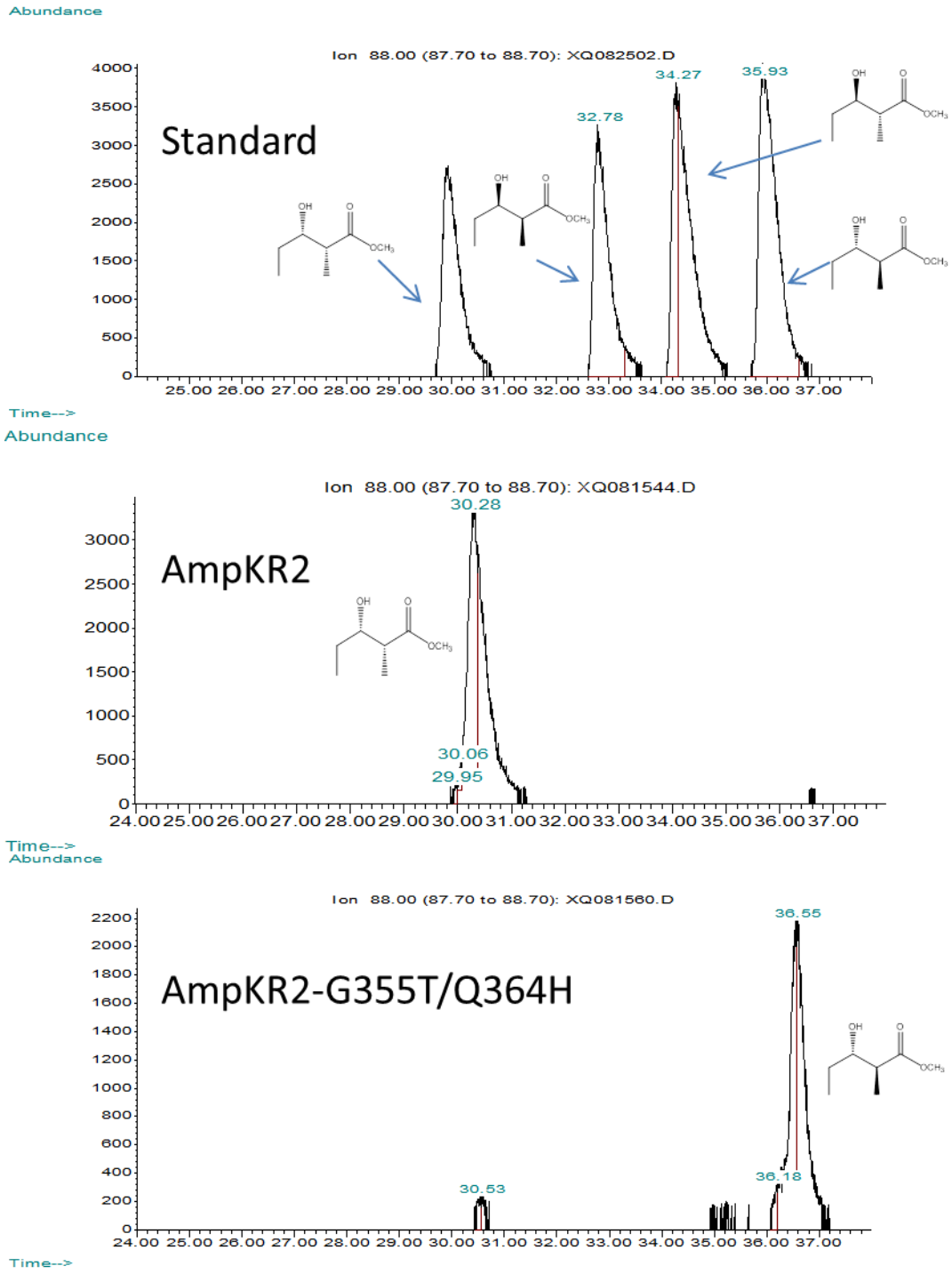

Figure S11. Chiral GC-MS analysis of the stereochemistry of diketide methyl esters derived from incubation of AmpKR2 and AmpKR2-G355T/Q364H with 2-methyl-3-ketopentanoyl-SNAC (**5**) and NADPH for 2 h at room temperature.

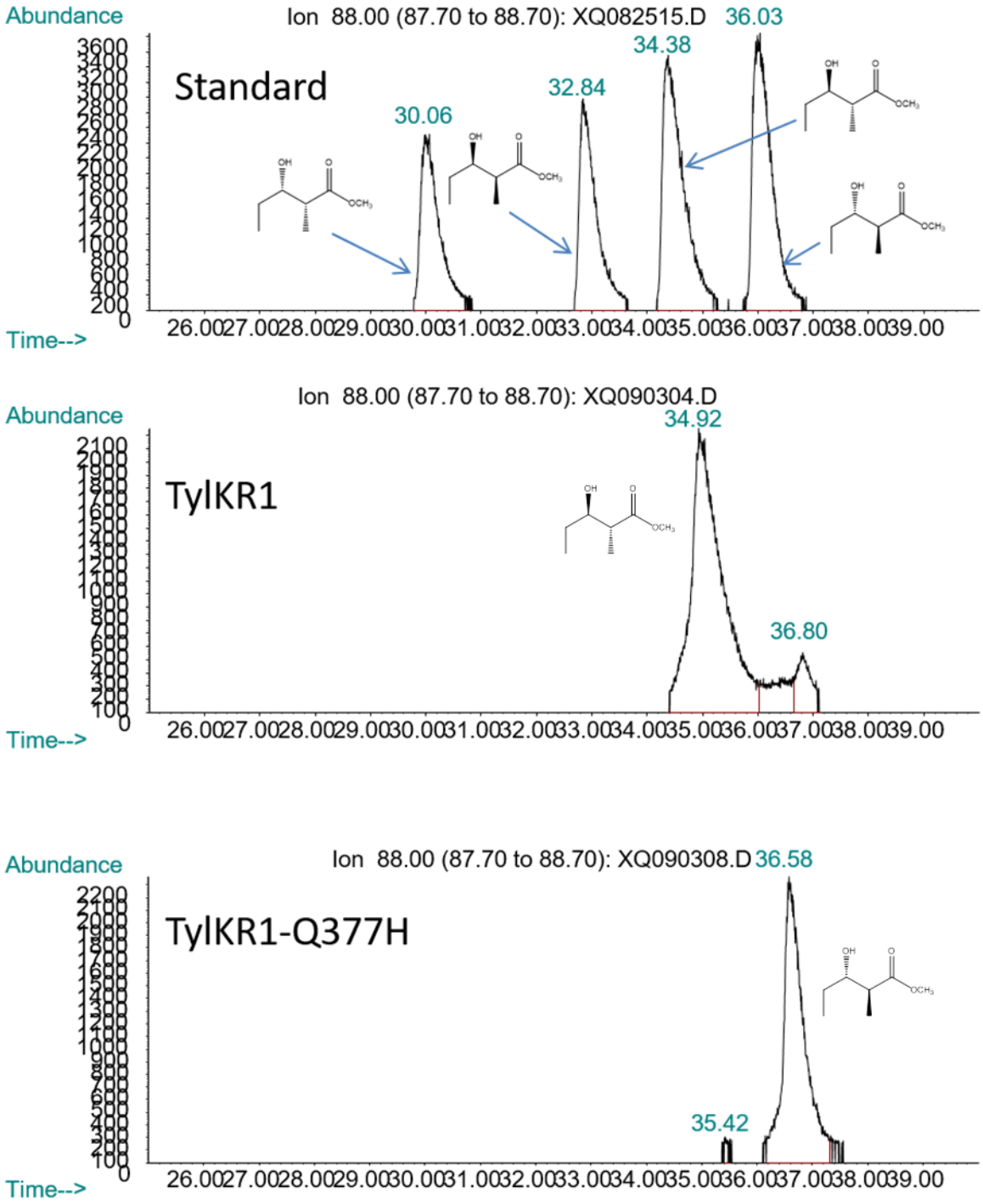

Figure S12. Chiral GC-MS analysis of the stereochemistry of diketide methyl esters derived from incubation of TylKR1 and TylKR1-Q377H with 2-methyl-3-ketopentanoyl-SNAC (**5**) as substrate and NADPH for 2 h at room temperature.

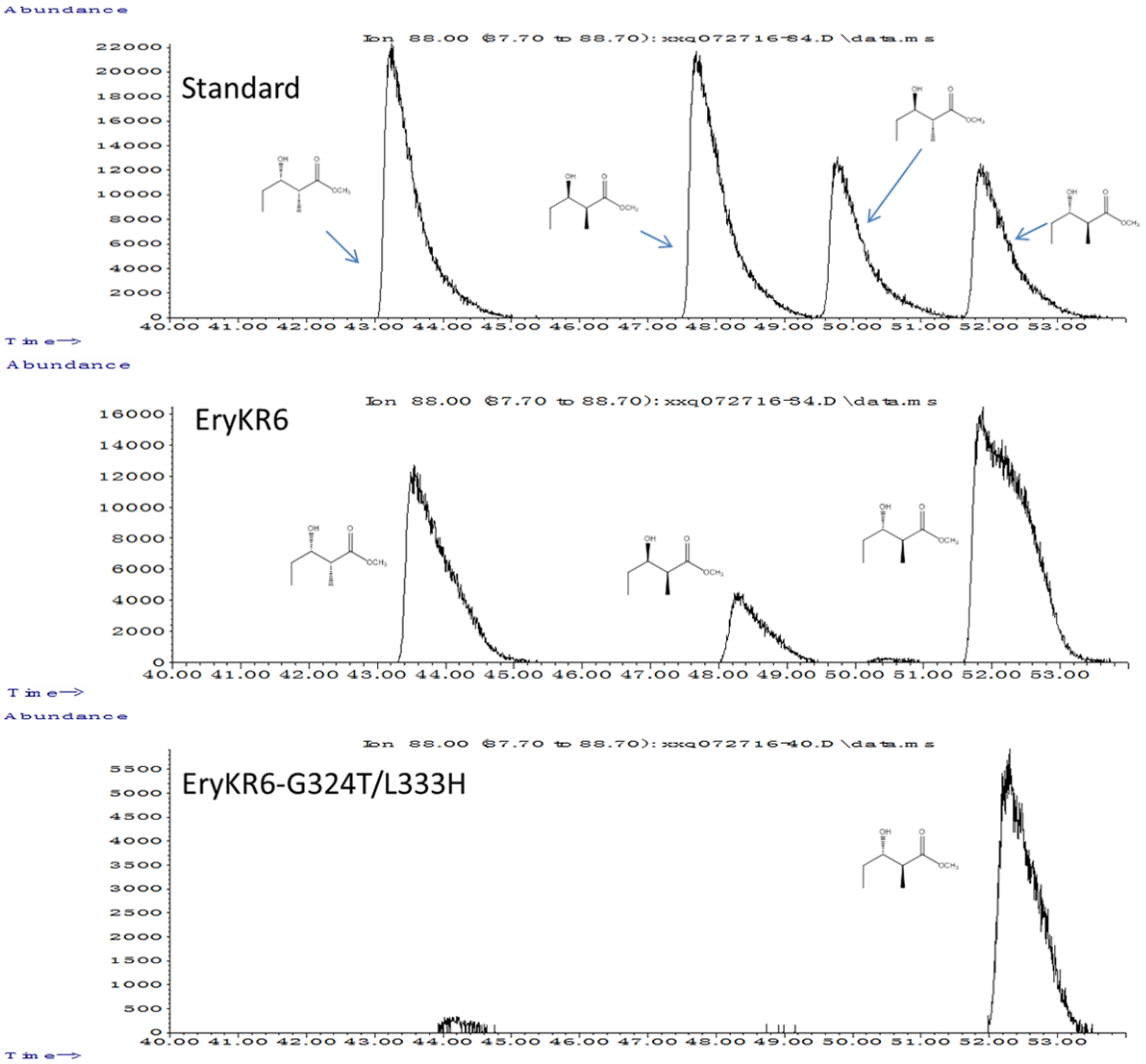

Figure S13. Chiral GC-MS analysis of the stereochemistry of diketide methyl esters derived from incubation of EryKR6 and EryKR6-G324T/L333Hwith 2-methyl-3-ketopentanoyl-SNAC (**5**) and NADPH for 2 h at room temperature.

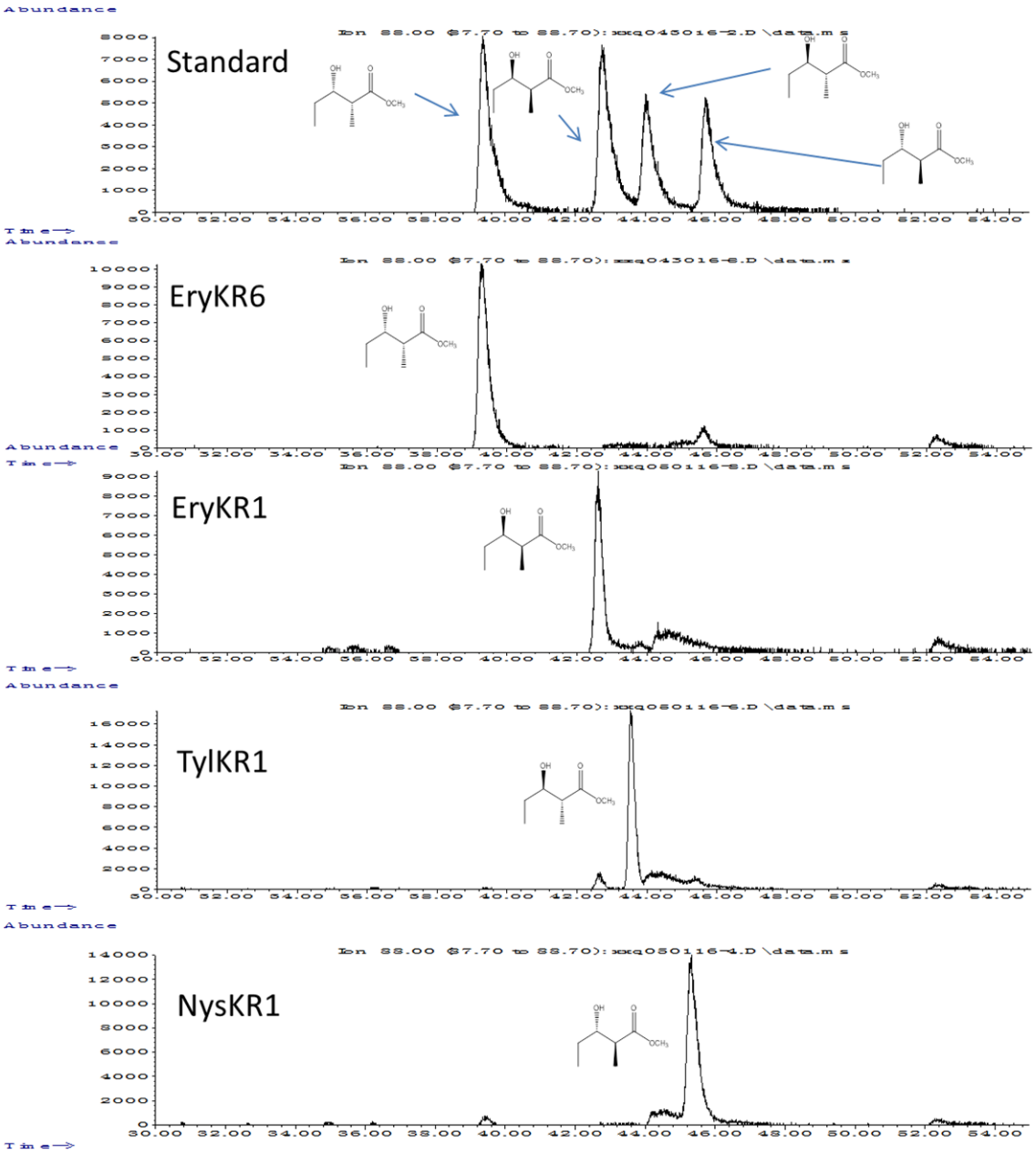

Figure S14. Chiral GC-MS analysis of methyl 2-methyl-3-hydroxypentanoates produced by KR-catalyzed reductions of 2-methyl-3-ketopentanoyl-NanACP1 (**7a**) generated *in situ* by incubation of Nan[KS1][AT1], propionyl-SNAC, *holo*-NanACP1, methylmalonyl-CoA and NADPH for 1 h.

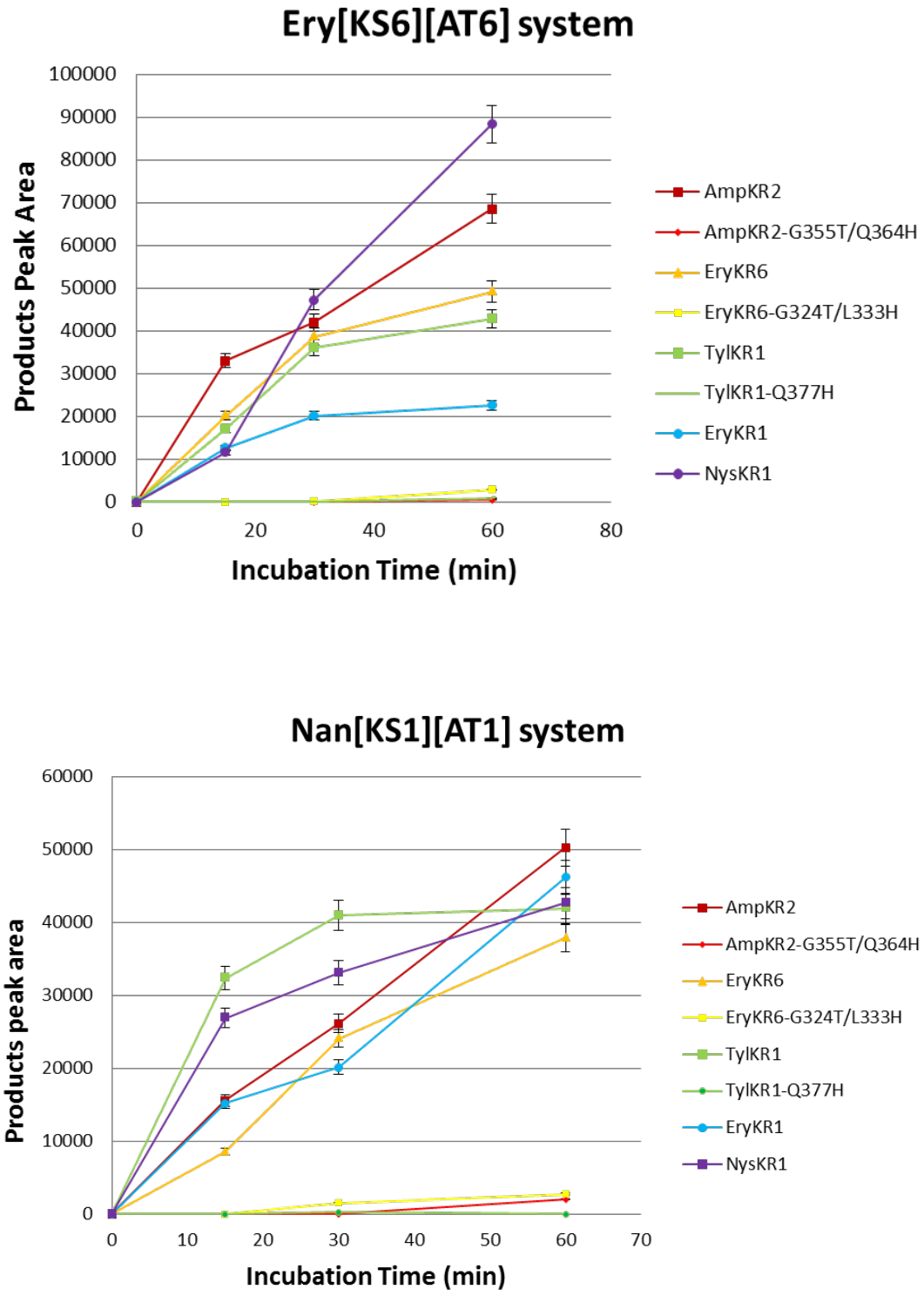

Figure S15. Kinetic analysis of recombinant KR domains incubated with reconstituted Ery[KS6][AT6] and EryACP6 or Nan[KS1][AT1] and NanACP1, based on GC-MS quantitation of derived diketide methyl esters. See Table S7 for summary of calculated rates of product formation for each KR domain.

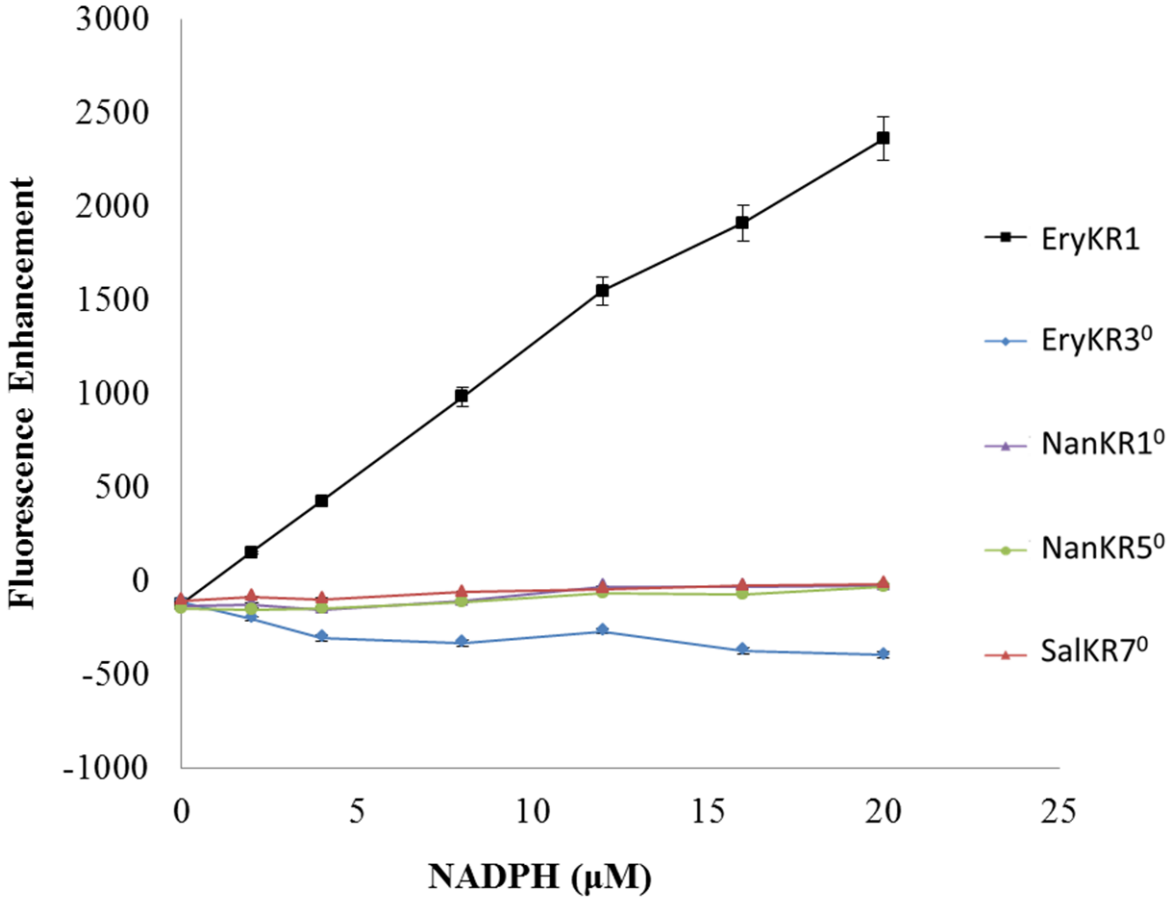

Figure S16. Fluorescence enhancement analysis of NADPH binding by NanKR1^0. The ketoreductase-active EryKR1 was used as a control in these experiments. NanKR5^0 and SalKR7^0. Proteins at 10 μM were titrated with increasing concentrations of NADPH. Cofactor fluorescence enhancement was determined as described in the Methods section.

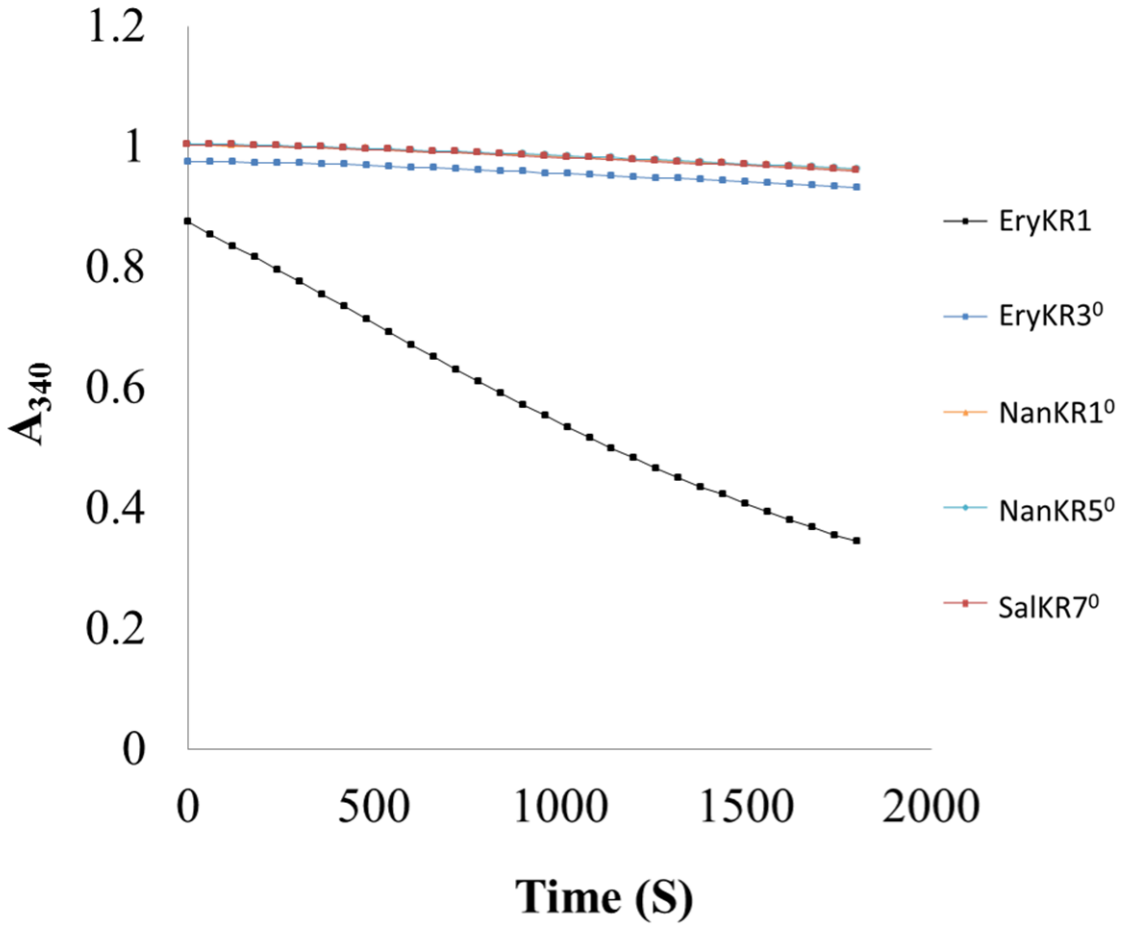

Figure S17. Absence of reductase activity of KR^0 domains. KR-catalyzed reduction of 8 mM (±)-2-methyl-3-ketopentanoyl-SNAC **(5)** by 5 μM $NanKR1^0$, $NanKR5^0$ and $SalKR7^0$, with monitoring of the consumption of NADPH by the absorbance at 340 nm. The ketoreductase-active EryKR1 was used as a positive control in these experiments, with redox-inactive $EryKR3^0$ serving as the negative control.

Table S1. Rare Codons in Nan[KS1][AT1]

Rare codons/total codons for one amino acid	Arg	Leu	Pro
Nan[KS1][AT1]	3/71	1/84	28/65

Table S2. Mutagenic Primers Utilized to Generate KR Mutants

Mutation	F or R	Primer Sequence; 5′-3′
EryKR6 outside primers	F	ATCGTAATCCATATGGCCGACAGCCGCTACCGCGTCGACTGGCGACCGC
	R	TGATTCGATGAATTCACGTCATCTCCCGCGCCGGGGCCGCCTGCACCGCGGGG
EryKR6-G324T	F	CGCCGAGACCTTCGTCCTGTTCTCGTCC**ACA**GCGGGGGTGTGGGGCAGTGCG
	R	CGCACTGCCCCACACCCCCGC**TGT**GGACGAGAACAGGACGAAGGTCTCGGCG
EryKR6-L333H	F	GCGGGGGTGTGGGGCAGTGCGAAC**CAC**GGCGCCTACTCCGCGGCCAACGCC
	R	GGCGTTGGCCGCGGAGTAGGCGCC**GTG**GTTCGCACTGCCCCACACCCCCGC
TylKR1 outside primers	F	GCAGATATACATATGAGCCCCACCGATGCCTGGCGC
	R	GTGGTGCTCGAGTCATCAGGCTGCCGTCAGGGCCTCCCG
TylKR1-Q377H	F	CCGGCACATGGGGCAACGCCGGC**CAC**GGTGCGTACGCCGCCGCCAACGCCG
	R	CGGCGTTGGCGGCGGCGTACGCACC**GTG**GCCGGCGTTGCCCCATGTGCCGG

F, forward primer; R, reverse primer. Bold letters represent the introduced mutant codons. restriction site underlined, stop codon colored.

Table S3. Mutagenic Primers for Generation of SalKR7^0 Mutants

Mutation	F or R	Primer Sequence; 5′-3′
SalKR7-F362Y	F	GGCGGCGAGCACGCGGCG**TAT**GCAGCCGCAAGCGC
	R	GCGCTTGCGGCTGC**ATA**CGCCGCGTGCTCGCCGCC
SalKR7-S349A	F	GGCATTCGTCCTGTTCAGC**GCC**GTTACCAGCTATTGGGG
	R	CCCCAATAGCTGGTAAC**GGC**GCTGAACAGGACGAATGCC

F, forward primer; R, reverse primer. Bold letters represent the introduced mutant codons.

Table S4. Predicted MW and observed ESI-MS M_D of recombinant KR domains and their mutants.

Protein	MW (cal, Da)	LC-QTOF (M_D, Da)
EryKR6-G324T	49299.66	49301.42
EryKR6- L333H	49298.64	49299.97
EryKR6-G324T/L333H	49342.69	49344.25
TylKR1-Q377H	53124.17	53125.92
NanKR1^0	48632.58	48633.0
NanKR5^0	47224.7	47225.7
SalKR7^0	52102.3	52103.4
SalKR7^0-F362Y	52118.3	52119.0
SalKR7^0-S349A	52086.3	52087.4
SalKR7^0-F362Y/ S349A	52102.3	52103.39

Table S5. Steady-state kinetic parameters for reduction of (±)-2-methyl-3-ketopentanoyl-SNAC (**5**) by wild-type and mutant KR proteins. See Figure S10 for plots of *V* vs [S] for each KR domain.

KR	k_{cat} (s^{-1})	K_m (mM)	k_{cat}/K_m ($mM^{-1}s^{-1}$)
EryKR6	0.086±0.001	23±8	0.0037
EryKR6-G324T/L333H	0.11±0.002	32±10	0.0034
TylKR1	0.44±0.04	10.9±2.8	0.040
TylKR1-Q377H	0.094±0.016	37±13	0.0025
AmpKR2	0.29±0.03	169.0±25	0.0017
AmpKR2-G355T/Q364H	0.18±0.01	18±3	0.0098

Table S6. Stereospecificity of the reduction of (±)-2-methyl-3-ketopentanoyl-SNAC (**5**) by wild-type and mutant ketoreductases and NADPH.

protein	diketide			
	2*R*,3*S* (%)	**2*S*,3*R* (%)**	**2*R*,3*R* (%)**	**2*S*,3*S* (%)**
TylKR1	0	0	91.3	8.7
TylKR1-Q377H	0	0	1.7	98.3
AmpKR2	100	0	0	0
AmpKR2-G355T/Q364H	2.3	0	0	97.7
EryKR6	35.2	12.2	0	52.6
EryKR6-G324T	6.9	6.2	0	86.9
EryKR6- L333H	25.9	0	0	74.1
EryKR6-G324T/L333H	0	0	0	100

Table S7. Kinetics of KR-catalyzed reduction of 2-methyl-3-ketopentanoyl-ACP generated *in situ* with Nan[KS1][AT1] plus NanACP1 or Ery[KS6][AT6] plus EryACP6. Relative values of k_{app}, derived from least-squares fits of GC-MS peak area of methyl 2-methyl-3-hydroxylpentanoate to $A_t = k_{app}*t$ for wild-type and mutant KR domains. See Figure S15 for plots of GC-MS peak area vs. time for each KS/KR combination.

Ery[KS6][AT6] system			**Nan[KS1][AT1] system**		
KR	**k_{app} (peak area•min^{-1})**	**$k_{app\text{-}mut}$/ $k_{app\text{-}wt}$**	**KR**	**k_{app} (peak area•min^{-1})**	**$k_{app\text{-}mut}$/ $k_{app\text{-}wt}$**
AmpKR2	1070±200		AmpKR2	880±40	
AmpKR2-G355T/Q364H	9.4±3.6	0.009	AmpKR2-G355T/Q364H	35±13	0.04
EryKR6	800±190		EryKR6	650±75	
EryKR6-G324T/L333H	49±17	0.06	EryKR6-G324T/L333H	50±10	0.07
TylKR1	700±190		TylKR1	610±330	
TylKR1-Q377H	14±6	0.02	TylKR1-Q377H	0.5±3	0.0007
EryKR1	355±125		EryKR1	745±70	
NysKR1	1540±160		NysKR1	640±220	

Table S8. Binding affinity of wild type SalKR7^0 and mutants for (±)-2-methyl-3-ketopentanoyl-SNAC (**5**).

Protein	K_d (mM)	K_d(mut)/ K_d(wt)
SalKR7^0	1.2	
SalKR7^0-F362Y	1.8	1.5
SalKR7^0-S349A	1.2	1.0
SalKR7^0-F362Y/ S349A	2.1	1.8

Table S9. Tandem EIX Assay of Redox-Inactive NanKR1^0 and NanKR5^0 Domains.

	time (min)					
	0	10	20	30	45	60
KR^0	Deuterium exchange of [2-^{2}H]-2 (%)[a]					
EryKR6	0	0	4	4	5	5
NanKR1^0	0	3	7	11	14	17
Nan KR5^0	0	7	11	13	15	19

[a]Average of two or more measurements (±2%)

Table S10. Tandem EIX Assay of Redox-Inactive SalKR7^0 and Mutant Domains.

	time (min)						
	0	10	20	30	40	50	60
KR^0	Deuterium exchange of [2-^{2}H]-2 (%)[a]						
EryKR6	0	0	4	4	5	7	7
SalKR7^0	0	4	9	20	24	26	29
SalKR7^0-F362Y	0	4	11	20	22	27	33
SalKR7^0-S349A	0	0	3	6	9	11	13
SalKR7^0-S349A/F362Y	0	4	9	13	15	17	17

[a]Average of two or more measurements (±2%)

Table S11. Tandem EIX data analysis. Relative values of k_{app} were calculated from least-squares fits of isotope exchange data to $\ln(A_t/A_0) = -k_{app}*t$ for wild-type and for mutant KR^0 domains, corrected for the rate of background exchange measured using EryKR6 alone (negative control).

KR	k_{app} **(min^{-1})**	k_{app} **(min^{-1}) (corr)**	k_{rel} **(%)**
SalKR7^0	0.0062	0.0049	100
SalKR7^0-F362Y	0.0067	0.0054	110
SalKR7^0-S349A	0.0026	0.0013	26
SalKR7^0-S349A/F362Y	0.0033	0.0020	41
EryKR6	0.0013	0	0

Supplemental Reference.

(1) Biasini, M.; Bienert, S.; Waterhouse, A.; Arnold, K.; Studer, G.; Schmidt, T.; Kiefer, F.; Cassarino, T. G.; Bertoni, M.; Bordoli, L.; Schwede, T. *Nucleic Acids Res* **2014**, *42*, W252-W258.